Supplementary Data

to

Synthesis and Characterization of Synthetically Useful Salts of the Weakly-Coordinating Dianion $[B_{12}Cl_{12}]^{2-}$

Vanessa Geis,[a] Kristin Guttsche,[a] Carsten Knapp,[*a] Harald Scherer,[a] Rabiya Uzun[a]

[a] *Institut für Anorganische und Analytische Chemie, Albert-Ludwigs Universität Freiburg, Albertstr. 21, 79104 Freiburg i. Br., Germany. E-mail: carsten.knapp@ac.uni-freiburg.de; Fax: +49-761-203-6001; Tel: +49-761-203-6150.*

1. Syntheses

1.1. Synthesis of $[NEt_3H]_2[B_{12}H_{12}]$.

1.1.1. A full experimental account. $Na[BH_4]$ (97.91 g, 2.599 mol) in diglyme (400 ml) was charged into a 1000 mL three-necked round bottom flask equipped with a 250 mL dropping funnel, which should reach under the surface of the reaction mixture, with a pressure equalizing sidearm, a reflux condenser and a bubbler containing silicon oil. Iodine (205.58 g, 0.810 mol) was dissolved in a minimal amount of diglyme (350 mL)[a] and added to the dropping funnel. The entire apparatus was flushed with dry argon. The suspension of $Na[BH_4]$ in diglyme was vigorously stirred and heated until the temperature rose to 100 °C.[b] Then iodine was added drop-wise over a period of 6 h.[c,d] During the addition the amount of insoluble $Na[BH_4]$ decreased and at the end a yellow color of the reaction mixture was observed. The dropping funnel was disassembled and the reaction mixture was continuously stirred over night at 100 °C under an atmosphere of argon to complete the formation of $[B_3H_8]^-$. On the next day the temperature was increased and the reaction mixture was refluxed (temperature of the oil bath was 185 °C) over night (16 h) under an atmosphere of dry argon to completely disproportionate $[B_3H_8]^-$ to $[B_{12}H_{12}]^{2-}$ and $[BH_4]^-$ (at this stage, usually, the yellow color disappeared and a white precipitate started to form). Eventually the reaction mixture was cooled down and the diglyme was distilled off under dynamic vacuum starting at 90 °C (oil bath) and increased to 140 °C after 1 hour.[e] A large amount of white solid ($Na_2[B_{12}H_{12}]$, $Na[BH_4]$, NaI) remained.[f] The white solid was dissolved in 600 mL of water (cloudy solution) and 280 mL of concentrated hydrochloric acid were added carefully to the

[a] Iodine dissolves very slowly in diglyme. However, vigorous stirring of the suspension for several hours (over night) dissolves the iodine completely.
[b] At temperatures higher 100 °C $[B_3H_8]^-$ decomposes and boron clusters start to form.
[c] A faster addition of iodine leads to reduced yields.
[d] During the addition of iodine hydrogen is formed, which escapes (together with some diborane) through the bubbler. The reaction should be carried out in a well vented fume hood.
[e] To reduce the costs the diglyme can be recycled by drying over CaH_2 followed by distillation.
[f] Previously it has been recommended to wash the solid reaction mixture with petrol ether to remove last traces of diglyme.[9] We did not find this additional step helpful.

solution (caution: hydrogen evolution). The acidified clear solution was stored in a fridge (+6 °C) over night and colorless crystals (ca. 15 g) of boric acid (Raman,[1] ^{11}B NMR) were formed and removed by filtration.[9] The filtrate was treated with 400 mL Et_3N (pH = 9-10) and readily a voluminous white solid precipitated.[g] The cloudy solution was stirred over night (14 h) to complete the precipitation.[h] The white solid (ca. 80 g) was collected by filtration. According to ^{11}B NMR the white solid still contained large amounts of boric acid.[i] Therefore the solid was suspended in water, heated, and then filtrated while still hot (50 and 60 °C) to remove the more soluble boric acid. The product was dried in vacuum to give $[NEt_3H]_2[B_{12}H_{12}]$ (28.50 g, 0.082 mol, 51%) as a white solid. $[NEt_3H]_2[B_{12}H_{12}]$ prepared according to this method was of high purity and did not contain any remaining boric acid or smaller boron clusters (e.g. $[B_6H_6]^{2-}$, $[B_{10}H_{10}]^{2-}$).

1.1.2. Discussion

The reaction proceeds in two steps. $[B_3H_8]^-$ is prepared in situ in the first step from $Na[BH_4]$ and I_2 and thermally decomposed in the second step to give $[B_{12}H_{12}]^{2-}$ as the main product.

a) Synthesis of intermediary $[B_3H_8]^-$. Numerous accounts on the reaction of $[BH_4]^-$ and I_2 have been published. Depending on the stoichiometry and reaction conditions different products are observed.[2] A small excess of I_2 causes further oxidation of the $[B_3H_8]^-$,[3] while a larger excess of I_2 (I_2 : $[BH_4]^- > 2$) results in the complete formation of BI_3.[4] A slight excess of $[BH_4]^-$ gives B_2H_6 as the main product.[5] A ratio of $[BH_4]^-$: $I_2 \geq 3{:}1$ yields $[B_3H_8]^-$ as the only product (Eq. 1).[6]

$$3\ NaBH_4 + I_2 \rightarrow NaB_3H_8 + 2\ NaI + 2\ H_2\uparrow \qquad \text{(Eq. 1)}$$

[g] Some authors suggested the addition of NEt_3•HCl to complete the precipitation of the product. We found this unnecessary.
[h] During stirring several colours appeared (white, pink, yellow).
[i] Note: ^{11}B NMR samples should be measured in D_2O to detect the boric acid.

Reactions optimized for the synthesis of $[B_3H_8]^-$ use a large excess of $[BH_4]^-$ (up to 1:6) to avoid any further oxidation of the anticipated reaction product $[B_3H_8]^-$.[6] However, a large excess of unreacted $Na[BH_4]$ would have to be carried on to the next reaction step. Thus, we used a 1:3 stochiometry with very little excess of $Na[BH_4]$. The $Na[BH_4]$ should be finely powdered and the dropping rate of I_2 in diglyme should be adjusted in a way that the I_2 reacts immediately after addition and no yellow color persists in the reaction mixture. This avoids further oxidation of the formed $[B_3H_8]^-$ by I_2.

b) Thermal decomposition of $[B_3H_8]^-$ to give $[B_{12}H_{12}]^{2-}$. In the second step the intermediate $[B_3H_8]^-$ is thermally decomposed to $[B_{12}H_{12}]^{2-}$ and $[BH_4]^-$ (Eq. 2).[7] This disproportionation reaction has been thoroughly investigated by different groups. It has been shown that $[B_{10}H_{10}]^{2-}$, $[B_6H_6]^{2-}$ and other boranates are formed as well.[8] Long reaction time and high temperature lead to the formation of $[B_{12}H_{12}]^{2-}$ as the main product.

$$5\ Na[B_3H_8] \rightarrow Na_2[B_{12}H_{12}] + 3\ Na[BH_4] + 8\ H_2\uparrow \qquad \text{(Eq. 2)}$$

c) Work-up and purification. Complete separation from the by-products $Na[BH_4]$ and NaI is necessary to obtain pure $[B_{12}H_{12}]^{2-}$. Hydrolysis with hydrochloric acid converts $[BH_4]^-$ to boric acid (Eq. 3), part of which is separated by filtration after storing the reaction mixture at +6 °C over night.[9]

$$Na[BH_4] + HCl + 3\ H_2O \rightarrow B(OH)_3 + NaCl + 4\ H_2\uparrow \qquad \text{(Eq. 3)}$$

The filtrate is neutralized with NEt_3. $[B_{12}H_{12}]^{2-}$ is quantitatively precipitated and separated by filtration (Eq. 4). The water soluble by-products NaI, and NaCl stay in solution. However, usually boric acid also precipitates and the purity of the isolated product should be checked by ^{11}B NMR.

$$Na_2[B_{12}H_{12}] + 2\ NEt_3{\bullet}HCl \rightarrow [HN(Et_3)]_2[B_{12}H_{12}]\downarrow + 2\ NaCl \qquad \text{(Eq. 4)}$$

For further reactions (e.g. halogenation of the $[B_{12}H_{12}]^{2-}$ cage) alkali metal salts of $[B_{12}H_{12}]^{2-}$ are preferred. These salts are easily obtained by neutralization with MOH (M = Li-Cs). The Cs^+ salt[10] is often preferred due to its low solubility in water,[11] and can be re-crystallized from boiling water. The more soluble alkali metal salts can be obtained by complete evaporation of the solvent in a polypropylene beaker.

$$[HN(Et_3)]_2[B_{12}H_{12}] + 2\ MOH \rightarrow M_2[B_{12}H_{12}] + 2\ [HN(Et_3)]OH \qquad \text{(Eq. 5)}$$

M = Li, Na, K, Cs

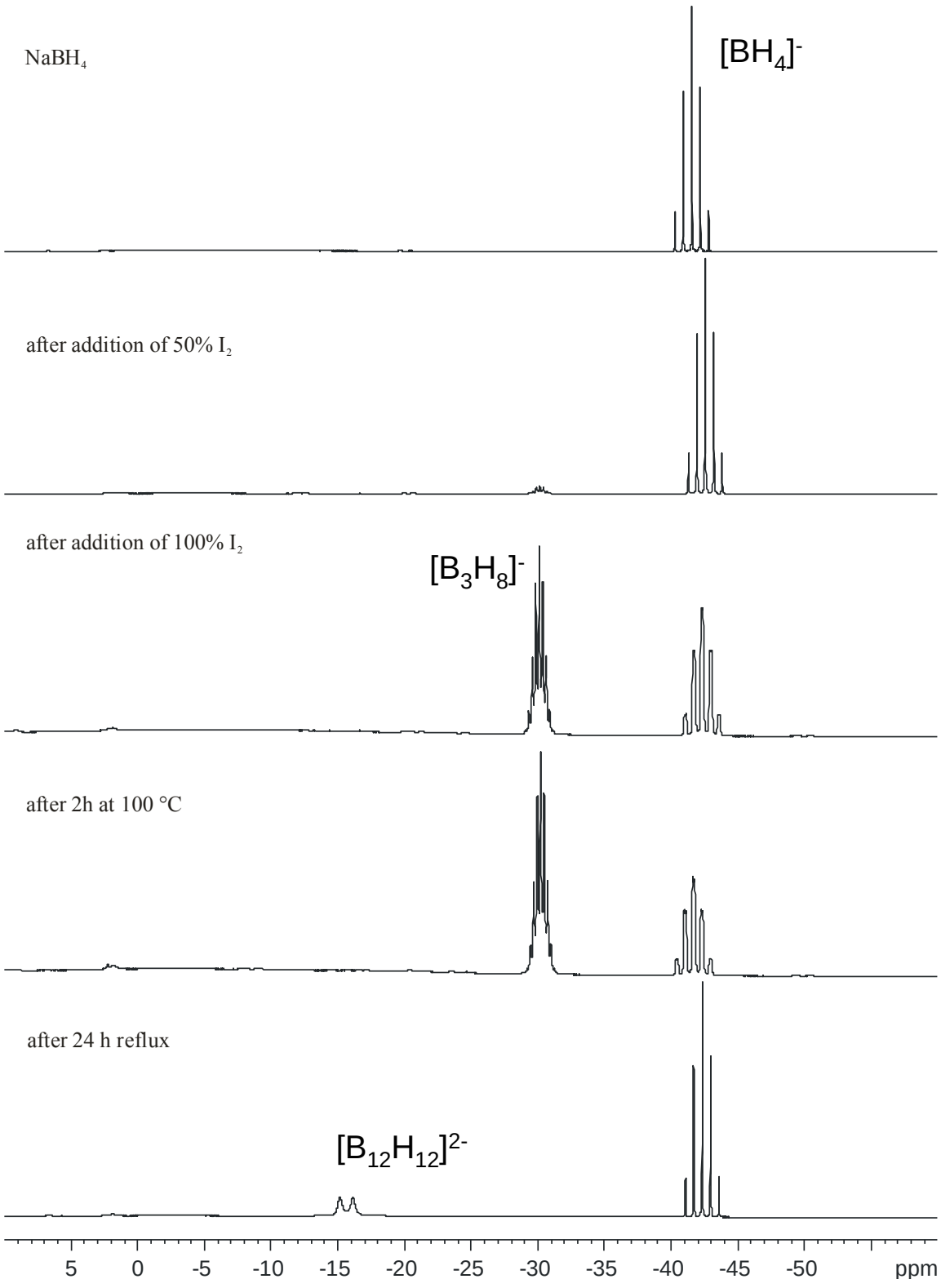

Fig. S1. ^{11}B NMR (CD_3CN, rt) spectra of samples taken at different steps in the $[B_{12}H_{12}]^{2-}$ synthesis.

1.2. Synthesis of $[B_{12}Cl_{12}]^{2-}$.

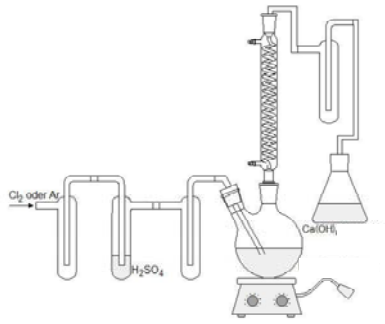

Fig. S2. Apparatus used for the chlorination of $[B_{12}H_{12}]^{2-}$.

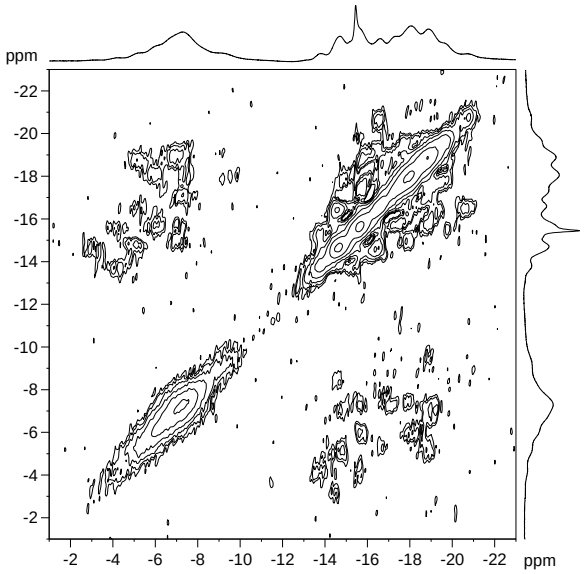

Fig. S3. ^{11}B-^{11}B-COSY (D_2O, rt, double quantum filtered, proton decoupled) of the reaction of $[B_{12}H_{12}]^{2-}$ with Cl_2 after 3 hours reaction time

The ^{11}B-^{11}B-COSY of the reaction of $[B_{12}H_{12}]^{2-}$ with Cl_2 after 3 hours reaction time at 0 °C is shown in figure S3. The range from -3 to -9 ppm corresponds to chlorine-bonded boron atoms and the range from -13 to -21 ppm to hydrogen-bonded boron atoms. The spectrum shows cross peaks between B-H and B-Cl groups as well as cross peaks between different B-H units but no cross peaks between different B-Cl groups. This is in agreement with chemically and magnetically equivalent B-Cl groups. The mixture contains only a limited number of species, which makes the chromatographic separation of the different species a promising task for future investigations.

2. Spectroscopic Data

2.1. $[NEt_3H]_2[B_{12}H_{12}]$

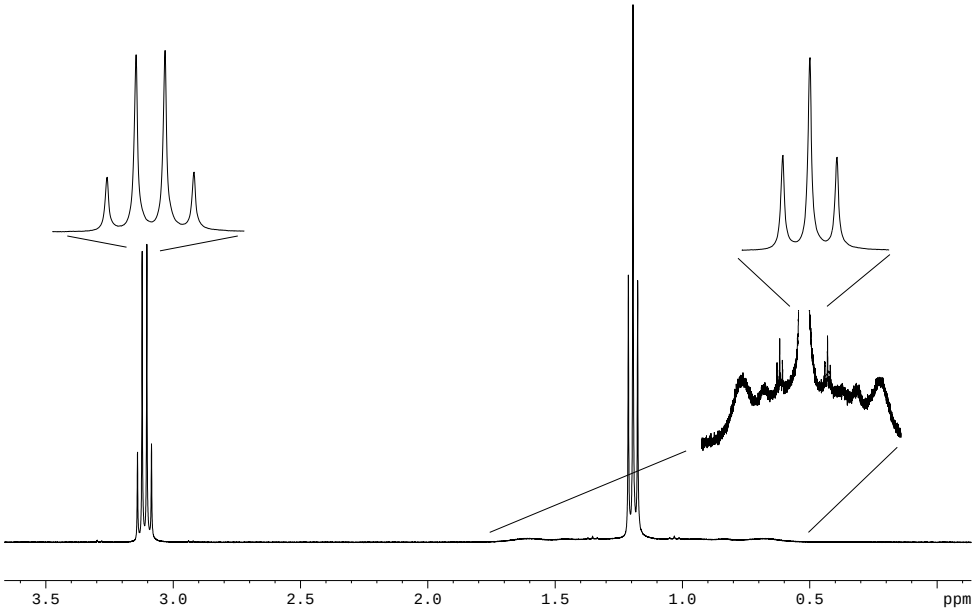

Fig. S4. ^{1}H NMR spectrum of $[NEt_3H]_2[B_{12}H_{12}]$ in D_2O at rt.

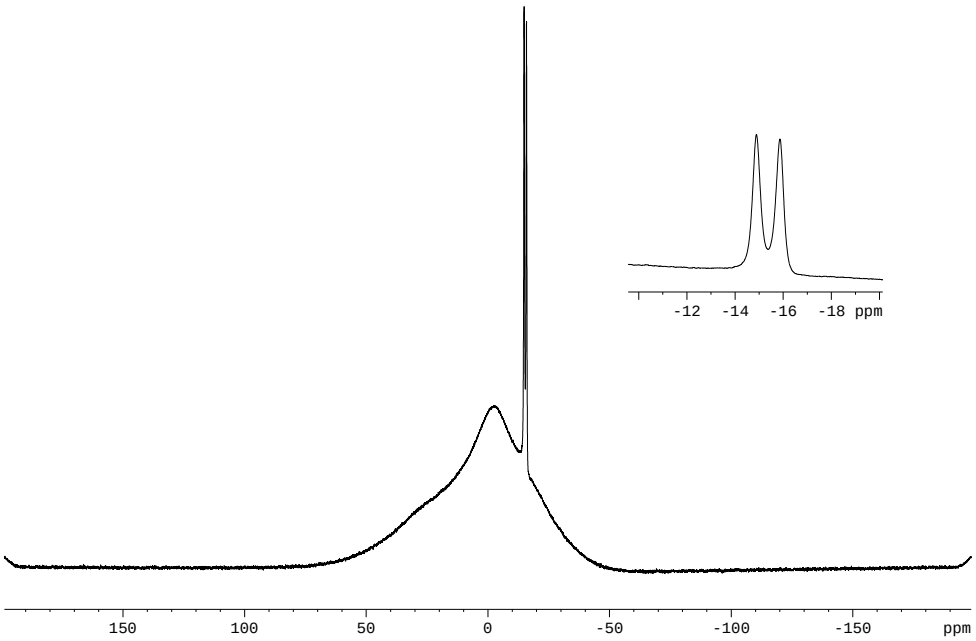

Fig. S5. ^{11}B NMR spectrum of $[NEt_3H]_2[B_{12}H_{12}]$ in D_2O at rt. The big hump is due to the boron in the glass of the NMR tube.

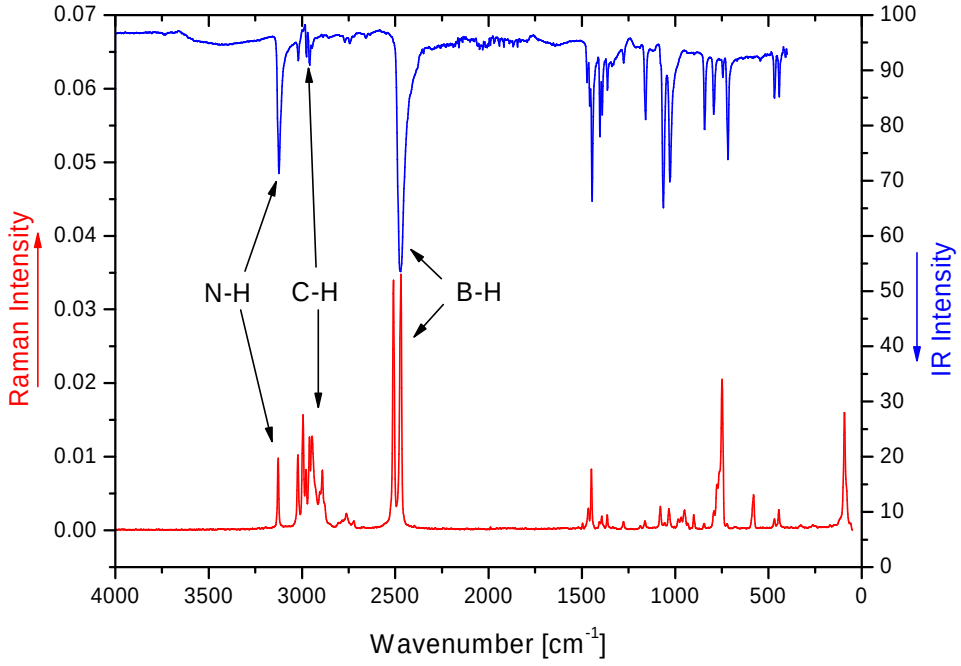

Fig. S6. IR (top, blue) and Raman (bottom, red, 50 mW, 2000 scans) spectra of $[NEt_3H]_2[B_{12}H_{12}]$.

2.2. $K_2[B_{12}H_{12}]$

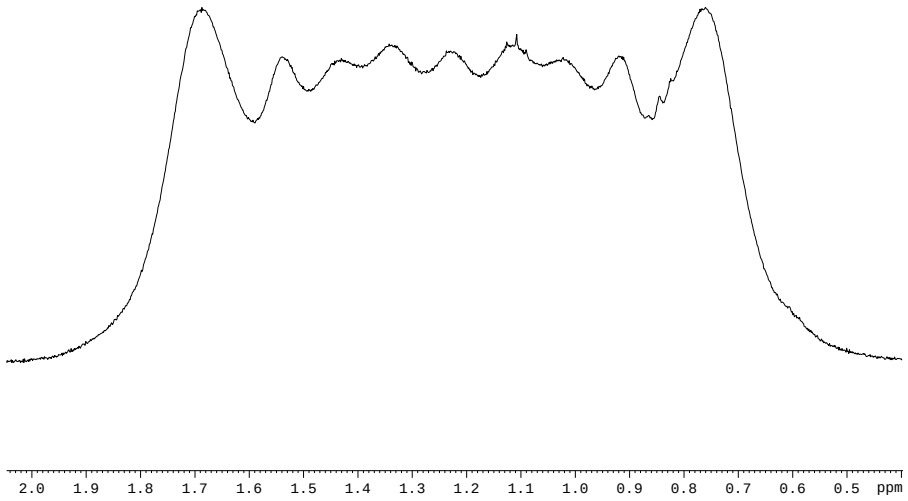

Fig. S7. ^{1}H NMR spectrum of $K_2[B_{12}H_{12}]$ in D_2O at rt showing the typical multiplet of $[B_{12}H_{12}]^{2-}$

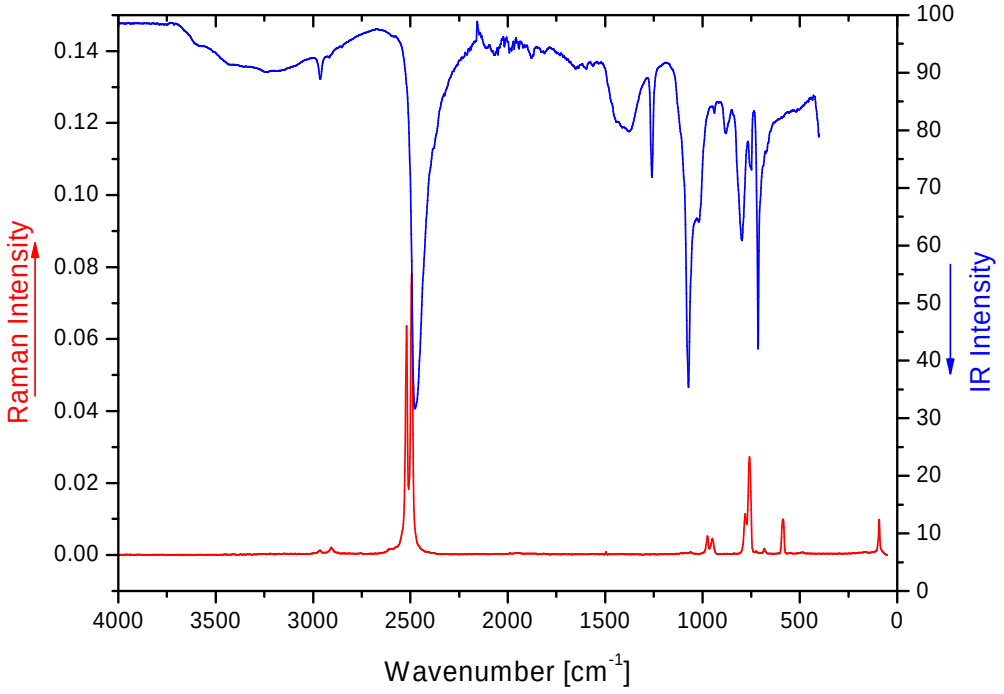

Fig. S8. IR (top, blue) and Raman (bottom, red, 50 mW, 2000 scans) spectra of $K_2[B_{12}H_{12}]$.

2.3. $Cs_2[B_{12}Cl_{12}]$

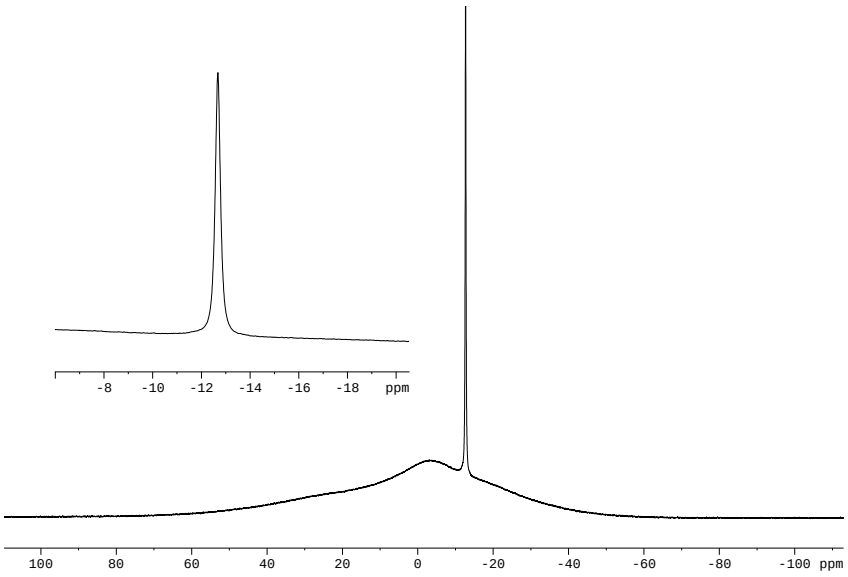

Fig. S9. ^{11}B NMR spectrum of $Cs_2[B_{12}Cl_{12}]$ in D_2O at rt. The big hump is due to the boron in the glass of the NMR tube. All alkali metal salts give essentially identical spectra.

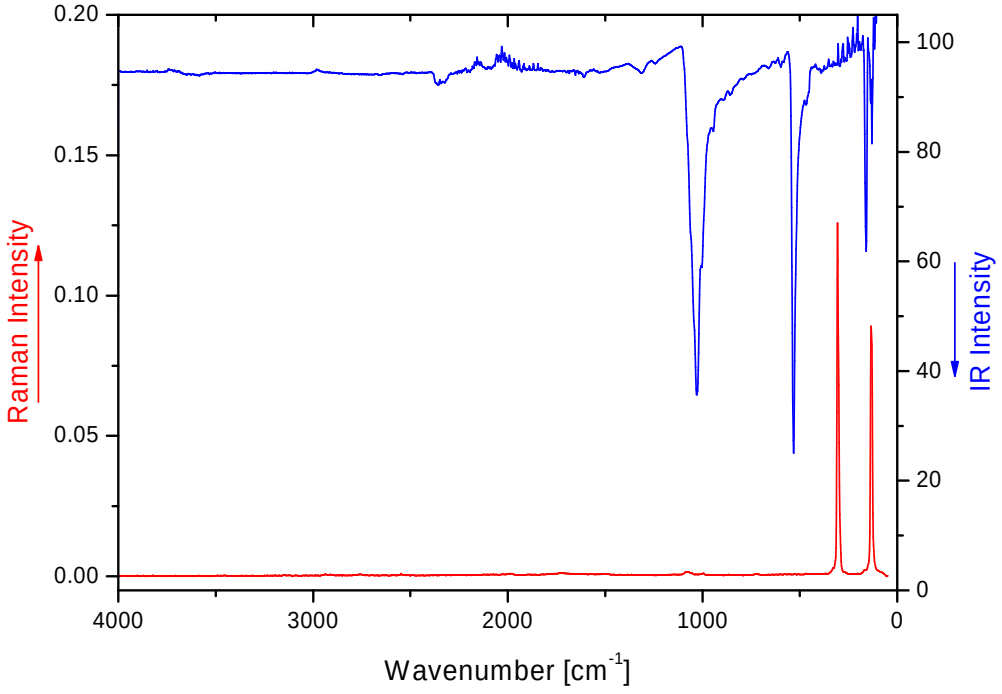

Fig. S10. IR and FIR (top, blue) and Raman (bottom, red) spectra of $Cs_2[B_{12}Cl_{12}]$. All alkali metal salts give essentially identical spectra.

2.4. $[NEt_3H]_2[B_{12}Cl_{12}]$

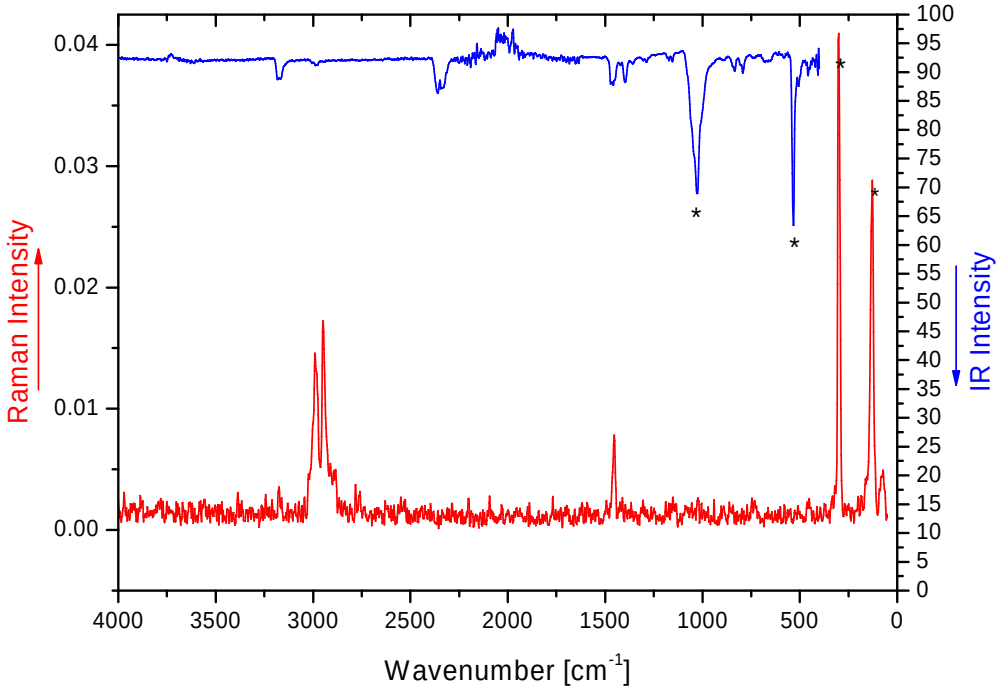

Fig. S11. IR (top, blue) and Raman (bottom, red) spectra of $[NEt_3H]_2[B_{12}Cl_{12}]$. Peaks marked with an asterisk belong to the $[B_{12}Cl_{12}]^{2-}$ anion.

2.5. $[NBu_4]_2[B_{12}Cl_{12}]$

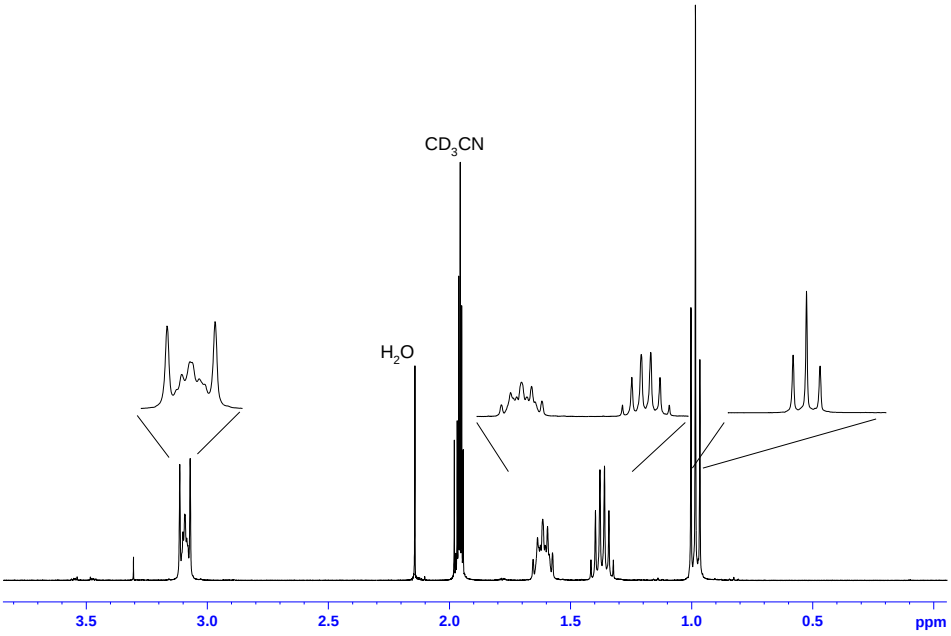

Fig. S12. ^{1}H NMR spectrum of $[NBu_4]_2[B_{12}Cl_{12}]$ in CD_3CN at rt.

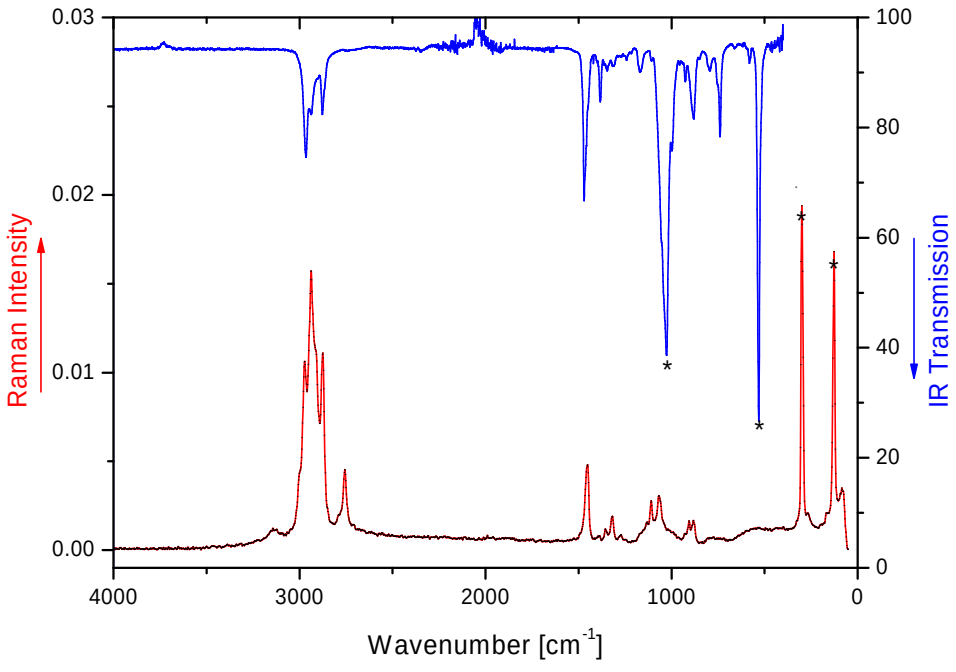

Fig. S13. IR (top, blue) and Raman (bottom, red) spectra of $[NBu_4]_2[B_{12}Cl_{12}]$. Peaks marked with an asterisk belong to the $[B_{12}Cl_{12}]^{2-}$ anion.

2.6. $[CPh_3]_2[B_{12}Cl_{12}]$

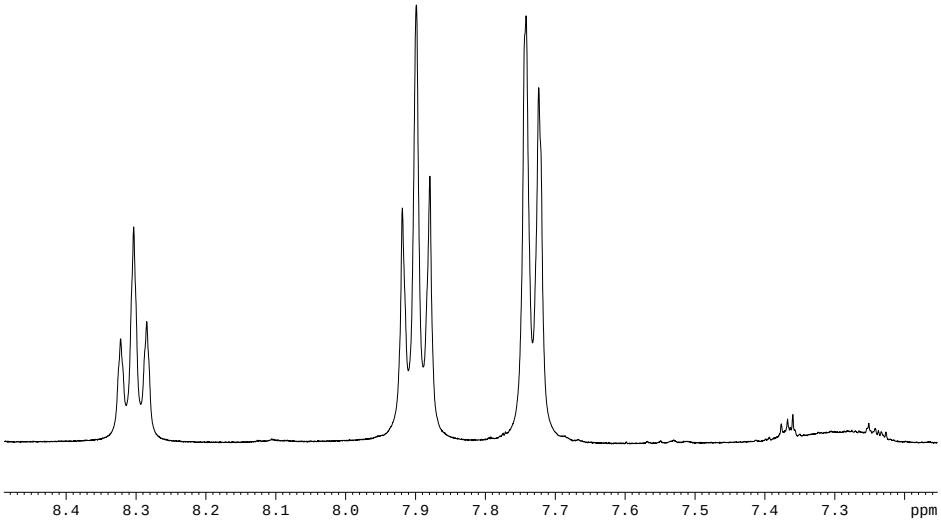

Fig. S14. ^{1}H NMR spectrum of $[CPh_3]_2[B_{12}Cl_{12}]$ in CD_3CN at rt.

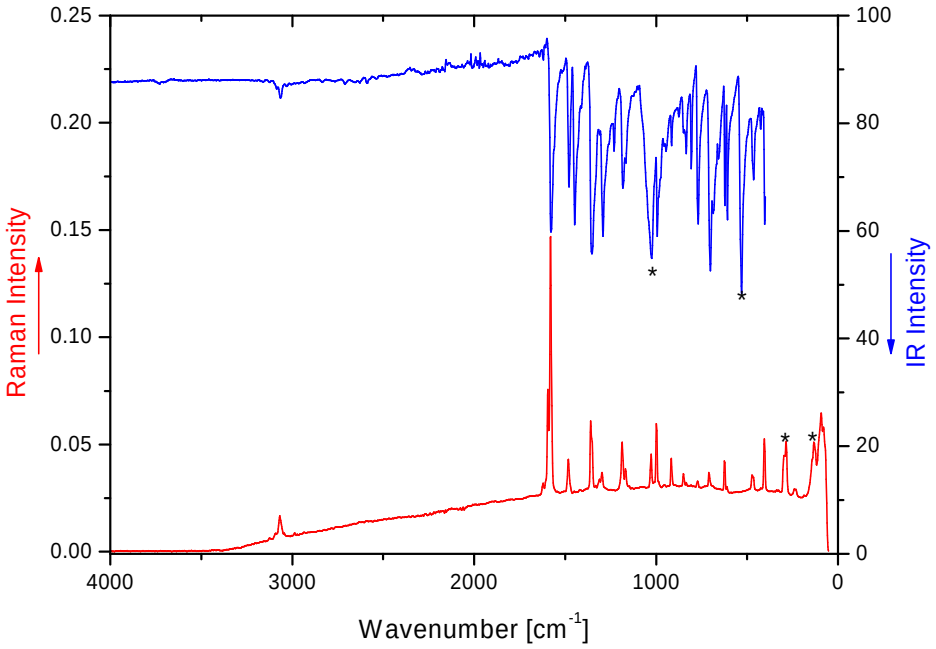

Fig. S15. IR (top, blue) and Raman (bottom, red) spectra of $[CPh_3]_2[B_{12}Cl_{12}]$. Peaks marked with an asterisk belong to the $[B_{12}Cl_{12}]^{2-}$ anion.

2.7. $[PPN]_2[B_{12}Cl_{12}]$

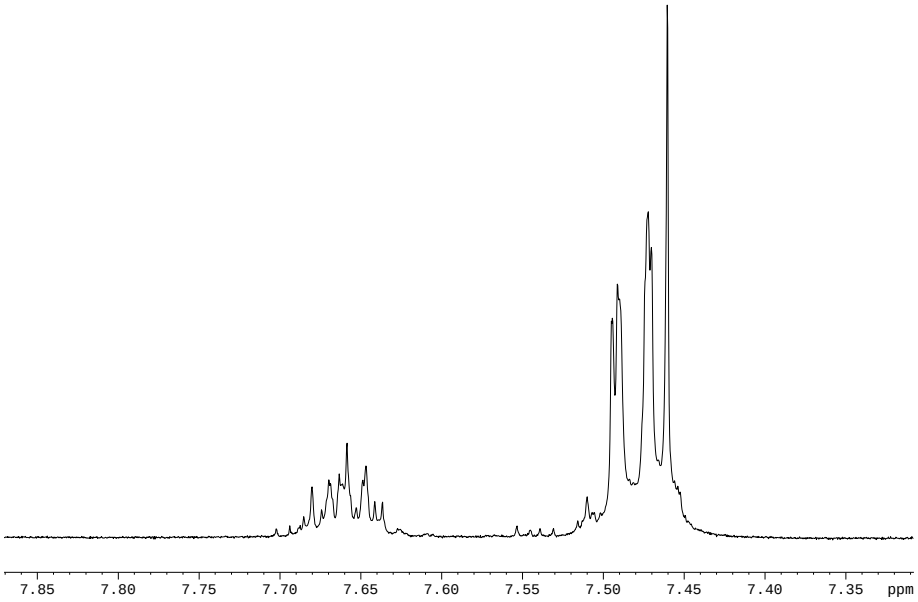

S16. ^{1}H NMR spectrum of $[PPN]_2[B_{12}Cl_{12}]$ in CD_2Cl_2 at rt

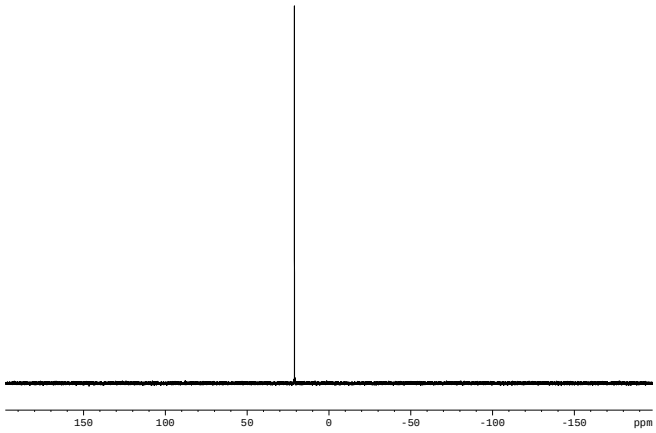

Fig. S17. ^{31}P NMR spectrum of $[PPN]_2[B_{12}Cl_{12}]$ in CD_2Cl_2 at rt

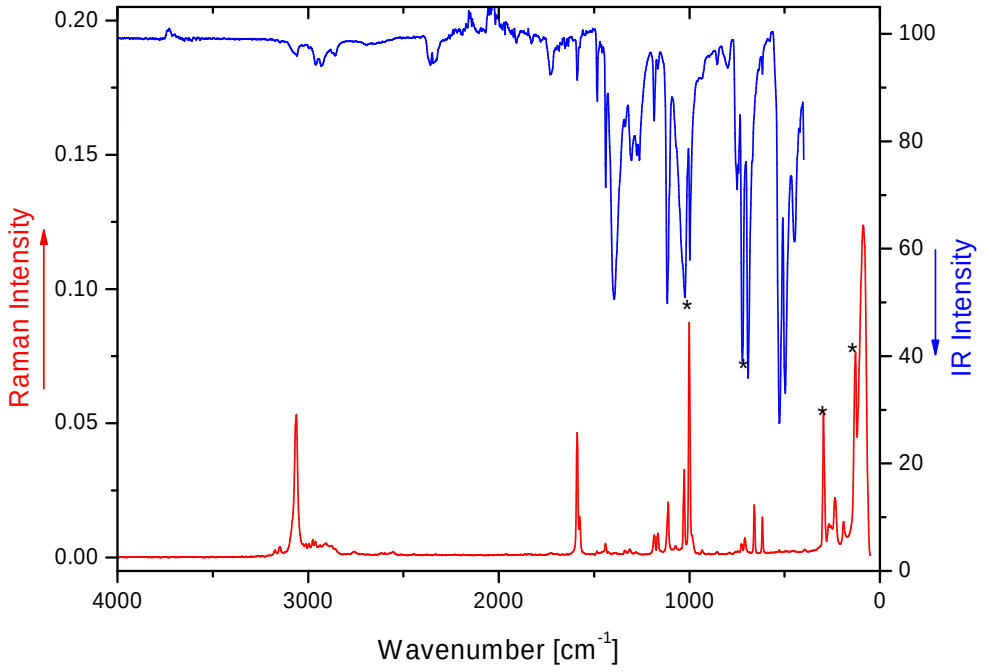

Fig. S18. IR (top, blue) and Raman (bottom, red) spectra of $[PPN]_2[B_{12}Cl_{12}]$. Peaks marked with an asterisk belong to the $[B_{12}Cl_{12}]^{2-}$ anion.

2.8. $[NO]_2[B_{12}Cl_{12}]$

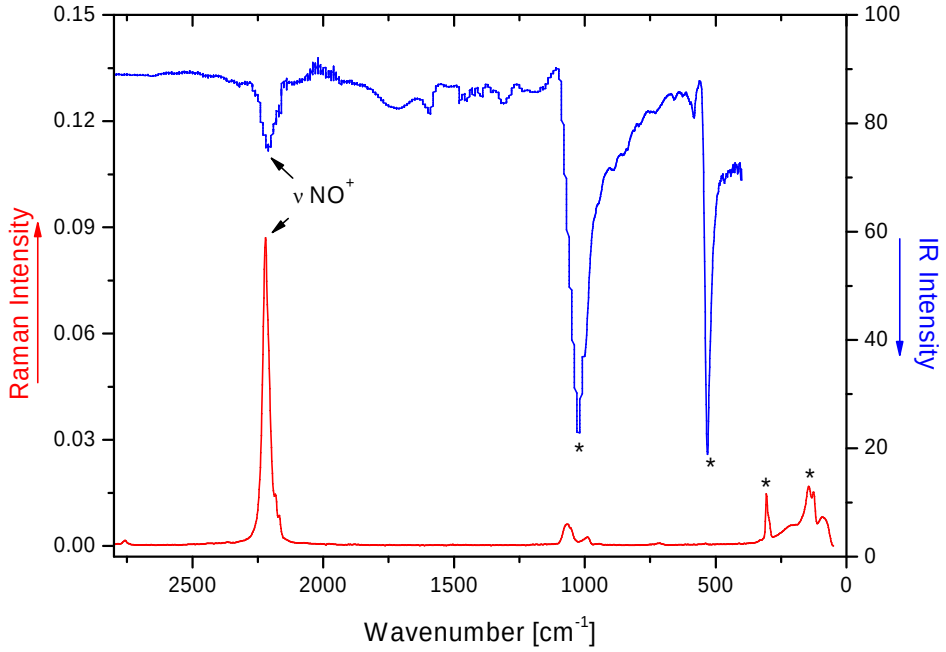

Fig. S19. IR (top, blue) and Raman (bottom, red) spectra of $[NO]_2[B_{12}Cl_{12}]$. Peaks marked with an asterisk belong to the $[B_{12}Cl_{12}]^{2-}$ anion.

3. Thermodynamics data

The thermodynamics for the formation of $[CPh_3]_2[B_{12}Cl_{12}]$ from CPh_3Cl and $Li_2[B_{12}Cl_{12}]$ in the solid state were investigated. Reaction enthalpies in the solid state were estimated by Born-Fajans-Haber cycles using the "volume-based" thermodynamics (VBT) approach to access lattice enthalpies (Table S1).[12] The total lattice potential energy, U_{pot} of a salt M_pX_q can be estimated from the formula unit volume, V_m, by:

$$U_{pot}(M_pX_q) = 2I\,(\alpha\, V_m^{-1/3} + \beta)$$

where V_m is the molecular volume (in nm^3), I is the lattice ionic strength, α and β are empirical constants. The sublimation enthalpy of Ph_3CCl of 114 kJ/mol was taken from ref. 13 The chloride affinity of Ph_3C^+ in the gas phase was calculated in an isodesmic reaction (energies in kJ/mol):

$H_3CCl \xrightarrow{+941} H_3C^+ + Cl^-$ G3[14]

$CPh_3Cl + H_3C^+ \xrightarrow{-514} CPh_3^+ + H_3CCl$ PBE0/QZVPP

$CPh_3Cl \xrightarrow{+427} CPh_3^+ + Cl^-$

Table S1 Molecular volumes [nm^3] and lattice enthalpies [kJ/mol]

	V_m	H_L	Ref.
$Li_2[B_{12}Cl_{12}]$	0.331[a]	1255	
LiCl		832	15
$[CPh_3]_2[B_{12}Cl_{12}]$	770[b]	772	

[a] Calculated from V_m of $Cs_2[B_{12}Cl_{12}]$ -2 $V(Cs^+)$ + 2 $V(Li^+)$ (taken from ref 16).

[b] Calculated from the averaged volumes taken from the crystal structures of **2** and **3** (volumes of the solvent molecules (taken from ref 17) were subtracted.

Table S2 Calculated total energies and zero point energies (ZPE)

Compound	Method	Total energy including ZPE (a.u.)
H_3CCl	G3	-499.913921
H_3C^+	G3	-39.430576
Cl^-	G3	-460.123600
H_3CCl	PBE0/QZVPP	-499.916049
H_3C^+	PBE0/QZVPP	-39.406395
CPh_3Cl	PBE0/QZVPP	-1192.272751
CPh_3^+	PBE0/QZVPP	-731.952984

4. Quantum chemical calculations on $[B_{12}Cl_{12}]^{2-}$

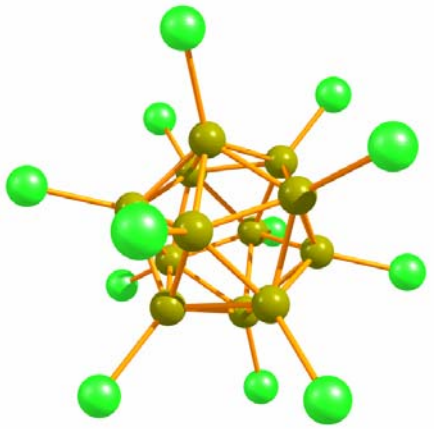

Table S3 Calculated B-B and B-Cl bond distances for $[B_{12}Cl_{12}]^{2-}$ at different levels

Method[18]	B-B Distance [pm]	B-Cl Distance [pm]	Total energy [a.u.]
BP86/SV(P)	180.2	182.2	-5820.149184297
PBE0/TZVPP	178.6	179.3	-5819.601632463
PBE0/QZVPP	178.6	179.3	-5819.778112098

Table S4 Calculated (BP86/SV(P)) vibrational data for $[B_{12}Cl_{12}]^{2-}$

mode	symmetry	wave number	IR intensity	selection rules	
		cm**(-1)	km/mol	IR	RAMAN
1		0.00	0.00000	-	-
2		0.00	0.00000	-	-
3		0.00	0.00000	-	-
4		0.00	0.00000	-	-
5		0.00	0.00000	-	-
6		0.00	0.00000	-	-
7	hu	105.55	0.00000	NO	NO
8	hu	105.55	0.00000	NO	NO
9	hu	105.55	0.00000	NO	NO
10	hu	105.55	0.00000	NO	NO
11	hu	105.55	0.00000	NO	NO
12	gg	111.32	0.00000	NO	NO
13	gg	111.32	0.00000	NO	NO
14	gg	111.32	0.00000	NO	NO
15	gg	111.32	0.00000	NO	NO
16	hg	114.80	0.00000	NO	YES
17	hg	114.80	0.00000	NO	YES
18	hg	114.80	0.00000	NO	YES
19	hg	114.80	0.00000	NO	YES
20	hg	114.80	0.00000	NO	YES
21	gu	116.63	0.00000	NO	NO
22	gu	116.63	0.00000	NO	NO
23	gu	116.63	0.00000	NO	NO
24	gu	116.63	0.00000	NO	NO
25	t1u	147.08	0.01260	YES	NO
26	t1u	147.08	0.01260	YES	NO
27	t1u	147.08	0.01260	YES	NO
28	hg	276.80	0.00000	NO	YES
29	hg	276.80	0.00000	NO	YES
30	hg	276.80	0.00000	NO	YES
31	hg	276.80	0.00000	NO	YES
32	hg	276.80	0.00000	NO	YES
33	ag	287.95	0.00000	NO	YES
34	t2u	301.74	0.00000	NO	NO
35	t2u	301.74	0.00000	NO	NO
36	t2u	301.74	0.00000	NO	NO
37	t1g	414.83	0.00000	NO	NO
38	t1g	414.83	0.00000	NO	NO
39	t1g	414.83	0.00000	NO	NO
40	t1u	520.21	97.95493	YES	NO
41	t1u	520.21	97.95493	YES	NO
42	t1u	520.21	97.95493	YES	NO
43	hu	583.88	0.00000	NO	NO
44	hu	583.88	0.00000	NO	NO
45	hu	583.88	0.00000	NO	NO
46	hu	583.88	0.00000	NO	NO
47	hu	583.88	0.00000	NO	NO
48	hg	696.83	0.00000	NO	YES
49	hg	696.83	0.00000	NO	YES
50	hg	696.83	0.00000	NO	YES
51	hg	696.83	0.00000	NO	YES
52	hg	696.83	0.00000	NO	YES
53	gg	731.76	0.00000	NO	NO
54	gg	731.76	0.00000	NO	NO
55	gg	731.76	0.00000	NO	NO
56	gg	731.76	0.00000	NO	NO
57	gu	771.99	0.00000	NO	NO

58	gu	771.99	0.00000	NO	NO
59	gu	771.99	0.00000	NO	NO
60	gu	771.99	0.00000	NO	NO
61	t2u	882.08	0.00000	NO	NO
62	t2u	882.08	0.00000	NO	NO
63	t2u	882.08	0.00000	NO	NO
64	hg	967.40	0.00000	NO	YES
65	hg	967.40	0.00000	NO	YES
66	hg	967.40	0.00000	NO	YES
67	hg	967.40	0.00000	NO	YES
68	hg	967.40	0.00000	NO	YES
69	t1u	1020.89	326.48632	YES	NO
70	t1u	1020.89	326.48632	YES	NO
71	t1u	1020.89	326.48632	YES	NO
72	ag	1036.99	0.00000	NO	YES

Table S5 Calculated (PBE0/TZVPP) coordinates for $[B_{12}Cl_{12}]^{2-}$

-2.32226136785382	1.68722164488970	-1.43523645609448	b
2.32226136785382	-1.68722164488970	1.43523645609448	b
0.00000000000000	0.00000000000000	-3.20928627961316	b
0.88702491175934	2.72998196798604	-1.43523645609448	b
-0.88702491175934	2.72998196798604	1.43523645609448	b
-2.87047291218897	0.00000000000000	1.43523645609448	b
-2.32226136785382	-1.68722164488970	-1.43523645609448	b
0.88702491175934	-2.72998196798604	-1.43523645609448	b
-0.88702491175934	-2.72998196798604	1.43523645609448	b
0.00000000000000	0.00000000000000	3.20928627961316	b
2.32226136785382	1.68722164488970	1.43523645609448	b
2.87047291218897	0.00000000000000	-1.43523645609448	b
-4.77472087121839	3.46903777229497	-2.95093978520648	cl
4.77472087121839	-3.46903777229497	2.95093978520648	cl
0.00000000000000	0.00000000000000	-6.59850195723031	cl
1.82378108601192	5.61302102383048	-2.95093978520648	cl
-1.82378108601192	5.61302102383048	2.95093978520648	cl
-5.90187957041295	0.00000000000000	2.95093978520648	cl
-4.77472087121839	-3.46903777229497	-2.95093978520648	cl
1.82378108601192	-5.61302102383048	-2.95093978520648	cl
-1.82378108601192	-5.61302102383048	2.95093978520648	cl
0.00000000000000	0.00000000000000	6.59850195723031	cl
4.77472087121839	3.46903777229497	2.95093978520648	cl
5.90187957041295	0.00000000000000	-2.95093978520648	cl

5. Structural Data

5.1. Preliminary crystal structure determination of $[NO]_2[B_{12}Cl_{12}]\cdot SO_2$

The $[NO]^+$ cations are disordered, probably resulting from several cation-anion contacts of almost equal energy and more space available than needed by $[NO]^+$. Therefore, nitrogen and oxygen atoms could not be distinguished crystallographically. Both $[NO]^+$ cations are surrounded by three $[B_{12}Cl_{12}]^{2-}$ anions each forming several contacts shorter than the sum of the van der Waals radii to $[NO]^+$ (see Fig. S21 and S22). Fig. S20 shows the unit cell of $[NO]_2[B_{12}Cl_{12}]\cdot SO_2$.

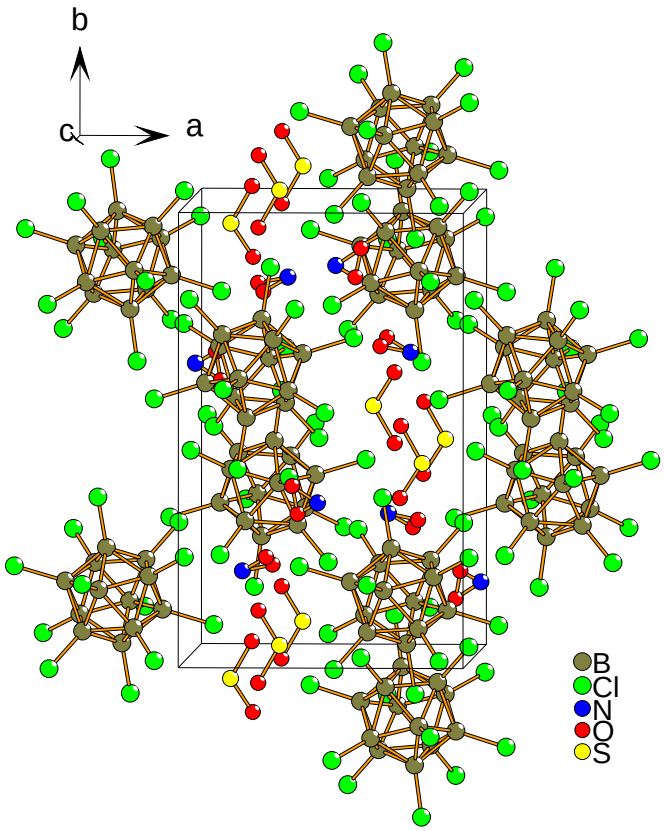

Fig. S20 Unit cell of $[NO]_2[B_{12}Cl_{12}]\cdot SO_2$. The $[NO]^+$ cations are disordered.

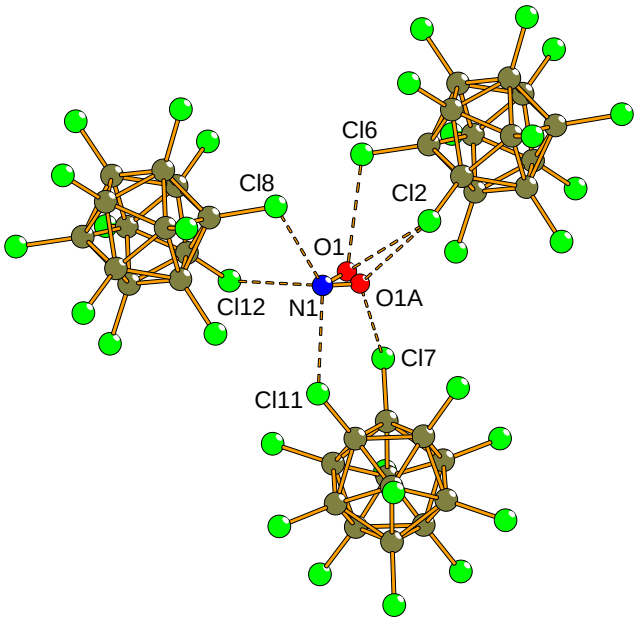

Fig. S21 Coordination sphere around $[NO]^+$_1 in $[NO]_2[B_{12}Cl_{12}]\cdot SO_2$. Selected cation-anion contacts [pm]: Cl2-O1 329, Cl6-O1 315, Cl2-O1A 303, Cl7-O1A 326, Cl8-N1 278, Cl11-N1 286, Cl12-N1 288.

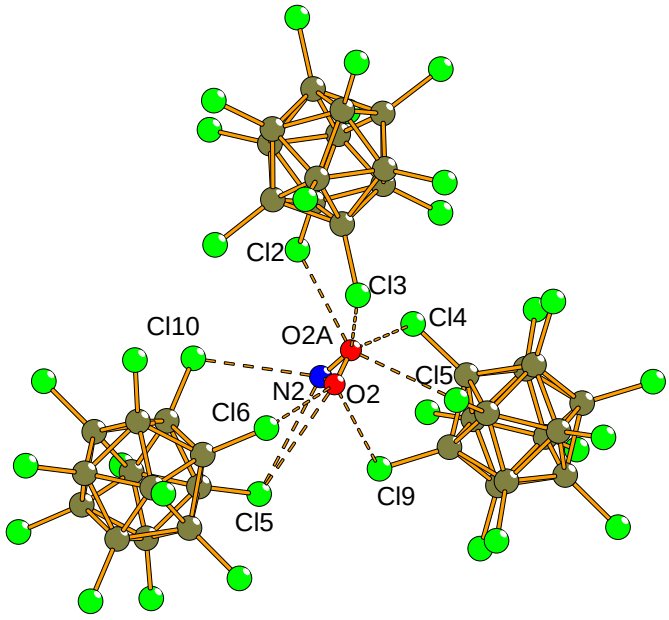

Fig. S22 Coordination sphere around $[NO]^+$_2 in $[NO]_2[B_{12}Cl_{12}]\cdot SO_2$. Selected cation-anion contacts [pm]: Cl2-O2A 282, Cl3-O2A 293, Cl4-O2A 275, Cl5-O2A 291, Cl9-O2 332, Cl5-O2 333, Cl6-O2 311, Cl5-N2 321, Cl10-N2 313.

Table S6 Crystal data and structure refinement for $[NO]_2[B_{12}Cl_{12}]\cdot SO_2$

Empirical formula	$B_{12}Cl_{12}N_2O_4S$	
Formula weight	679.20	
Temperature	113(2) K	
Wavelength	71.073 pm	
Crystal system	Orthorhombic	
Space group	$P2_12_12_1$	
Unit cell dimensions	a = 950.23(19) pm	$\alpha = 90°$
	b = 1521.8(3) pm	$\beta = 90°$
	c = 1575.8(3) pm	$\gamma = 90°$
Volume	2.2787(8) nm^3	
Z	4	
Density (calculated)	1.980 Mg/m^3	
Absorption coefficient	1.565 mm^{-1}	
F(000)	1304	
Crystal size	0.44 × 0.30 × 0.13 mm^3	
θ range for data collection	3.36 to 27.46°	
Index ranges	$-11 \le h \le 12$, $-19 \le k \le 18$, $-20 \le l \le 15$	
Reflections collected	8862	
Independent reflections	4776 [R(int) = 0.0285]	
Completeness to $\theta = 27.46°$	93.3 %	
Absorption correction	Semi-empirical from equivalents	
Max. and min. transmission	0.8224 and 0.5459	
Refinement method	Full-matrix least-squares on F^2	
Data / restraints / parameters	4776 / 0 / 288	
Goodness-of-fit on F^2	1.109	
Final R indices [$I>2\sigma(I)$]	R_1 = 0.0331, wR_2 = 0.0706	
R indices (all data)	R_1 = 0.0375, wR_2 = 0.0736	
Absolute structure parameter	-0.09(10)	
Largest diff. peak and hole	0.760 and -0.720 e.$Å^{-3}$	

Table S7 Atomic coordinates (x 10^4) and equivalent isotropic displacement parameters (pm^2x 10^{-1}) for $[NO]_2[B_{12}Cl_{12}]\cdot SO_2$. U(eq) is defined as one third of the trace of the orthogonalized U^{ij} tensor.

	x	y	z	U(eq)
B(1)	6471(5)	684(3)	7871(3)	11(1)
Cl(1)	5334(1)	-120(1)	8340(1)	19(1)
B(2)	6289(5)	999(3)	6792(3)	12(1)
Cl(2)	4946(1)	551(1)	6117(1)	16(1)
B(3)	7789(5)	386(3)	7124(3)	13(1)
Cl(3)	8062(1)	-735(1)	6811(1)	19(1)
B(4)	8283(5)	775(3)	8152(3)	13(1)
Cl(4)	9074(1)	94(1)	8948(1)	18(1)
B(5)	7084(5)	1624(3)	8449(3)	11(1)
Cl(5)	6594(1)	1799(1)	9533(1)	16(1)
B(6)	5847(5)	1770(3)	7605(3)	13(1)
Cl(6)	4070(1)	2108(1)	7797(1)	19(1)
B(7)	7997(5)	1273(3)	6384(3)	12(1)
Cl(7)	8451(1)	1096(1)	5303(1)	17(1)
B(8)	9229(5)	1137(3)	7244(3)	11(1)
Cl(8)	11013(1)	792(1)	7071(1)	19(1)
B(9)	8801(5)	1905(3)	8053(3)	12(1)
Cl(9)	10111(1)	2362(1)	8732(1)	16(1)
B(10)	7292(5)	2512(3)	7715(3)	11(1)
Cl(10)	7018(1)	3639(1)	8030(1)	17(1)
B(11)	6803(5)	2127(3)	6693(3)	12(1)
Cl(11)	5988(1)	2834(1)	5928(1)	17(1)
B(12)	8619(5)	2215(3)	6968(3)	12(1)
Cl(12)	9736(1)	3013(1)	6476(1)	20(1)
N(1)	8091(8)	6905(4)	9220(4)	71(2)
O(1)	7246(7)	7217(4)	9037(4)	23(1)
O(1A)	7039(9)	7040(6)	9327(6)	21(2)
N(2)	4848(6)	3603(5)	9524(5)	46(2)
O(2)	4141(9)	3355(6)	9367(5)	54(2)
O(2A)	3961(19)	3974(10)	9559(8)	34(4)
S(1)	8562(1)	4501(1)	9955(1)	31(1)
O(3)	7815(4)	5322(2)	9917(2)	36(1)
O(4)	7803(5)	3752(3)	10210(3)	59(1)

5.2. Preliminary crystal structure determination of $[PPN]_2[B_{12}Cl_{12}]\cdot CH_2Cl_2$

The crystal structure of $[PPN]_2[B_{12}Cl_{12}]\cdot CH_2Cl_2$ contains well defined $[B_{12}Cl_{12}]^{2-}$ anions, $[PPN]^+$ cations disordered equally over three position and disordered CH_2Cl_2 solvent molecules. Figure S23 shows a part of the crystal structure, figure S24 shows the unit cell.

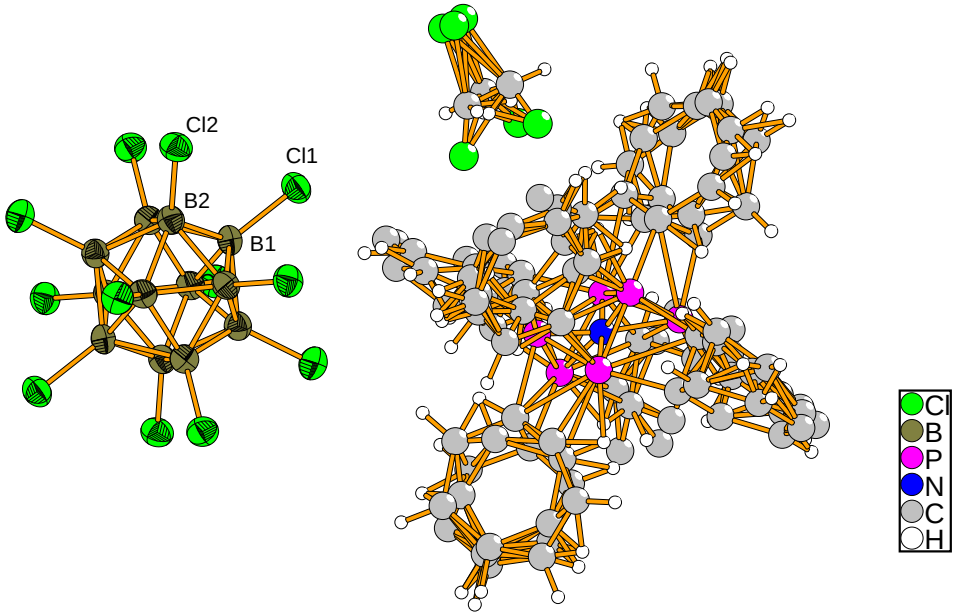

Fig. S23 Part of the crystal structure of $[PPN]_2[B_{12}Cl_{12}]\cdot CH_2Cl_2$. The structure contains $[B_{12}Cl_{12}]^{2-}$ anions, $[PPN]^+$ cations disordered over three positions, and disordered CH_2Cl_2 solvent molecules.

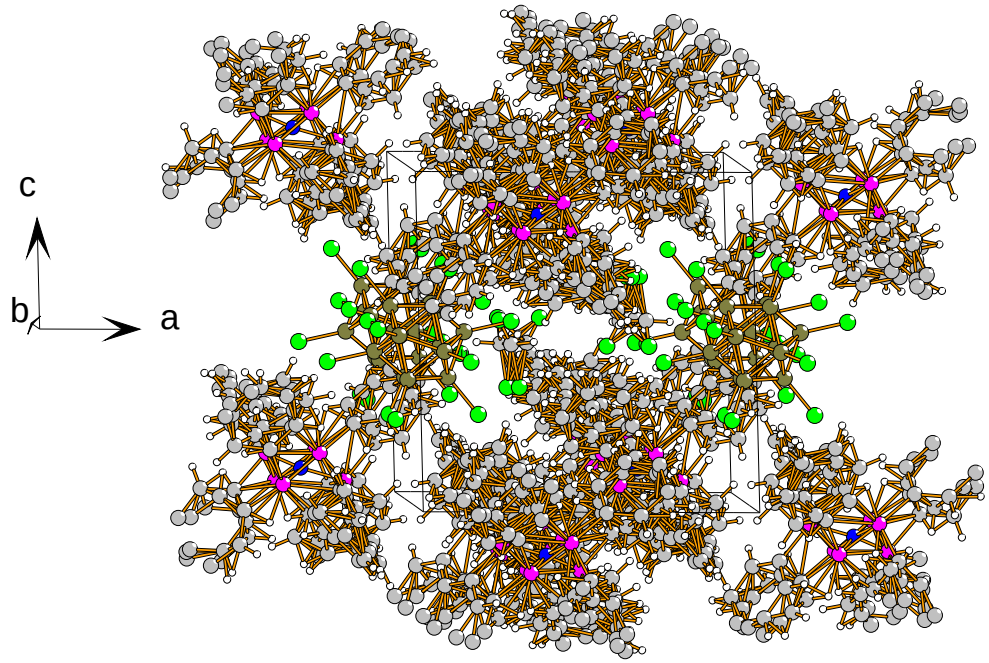

Fig. S24 Unit cell of $[PPN]_2[B_{12}Cl_{12}]$ showing the packing of $[B_{12}Cl_{12}]^{2-}$ anions and $[PPN]^+$ cations.

Table S8 Crystal data and structure refinement for $[PPN]_2[B_{12}Cl_{12}]\cdot CH_2Cl_2$

Empirical formula	$C_{74}H_{64}B_{12}Cl_{16}N_2P_4$	
Formula weight	1802.07	
Temperature	113(2) K	
Wavelength	71.073 pm	
Crystal system	Trigonal	
Space group	$P\bar{3}$	
Unit cell dimensions	a = 1379.4(2) pm	α = 90°
	b = 1379.4(2) pm	β = 90°
	c = 1261.3(3) pm	γ = 120°
Volume	2.0784(6) nm^3	
Z	1	
Density (calculated)	1.440 Mg/m^3	
Absorption coefficient	0.649 mm^{-1}	
F(000)	914	
Crystal size	0.18 × 0.17 × 0.10 mm^3	
θ range for data collection	3.23 to 22.58°	
Index ranges	$-14 \le h \le 14$, $-14 \le k \le 14$, $-13 \le l \le 13$	
Reflections collected	18471	

Independent reflections	1835 [R(int) = 0.0713]
Completeness to θ = 22.58°	99.3 %
Absorption correction	Semi-empirical from equivalents
Max. and min. transmission	0.9379 and 0.8921
Refinement method	Full-matrix least-squares on F^2
Data / restraints / parameters	1835 / 0 / 346
Goodness-of-fit on F^2	1.030
Final R indices [I>2σ(I)]	R_1 = 0.0355, wR_2 = 0.0760
R indices (all data)	R_1 = 0.0487, wR_2 = 0.0812
Largest diff. peak and hole	0.222 and -0.252 e.Å^{-3}

Table S9 Atomic coordinates (x 10^4) and equivalent isotropic displacement parameters (pm^{2}x 10^{-1}) for $[PPN]_2[B_{12}Cl_{12}]\cdot CH_2Cl_2$. U(eq) is defined as one third of the trace of the orthogonalized U^{ij} tensor.

	x	y	z	U(eq)
Cl(1)	1461(1)	2863(1)	4481(1)	43(1)
Cl(2)	901(1)	1777(1)	7190(1)	43(1)
B(1)	712(3)	1396(2)	4751(3)	34(1)
B(2)	436(3)	861(3)	6072(3)	35(1)
P(1)	6027(2)	1982(2)	675(2)	33(1)
N(1)	6667	3333	1078(4)	62(1)
P(2)	7194(2)	2803(2)	1546(2)	33(1)
C(1)	6934(6)	1737(6)	-152(5)	36(2)
C(2)	7006(7)	776(6)	-71(6)	57(3)
C(3)	7706(9)	615(9)	-741(8)	69(4)
C(4)	8334(11)	1415(11)	-1493(9)	57(9)
C(5)	8262(10)	2377(10)	-1574(10)	63(7)
C(6)	7561(7)	2538(7)	-904(7)	53(3)
C(1A)	8252(13)	3080(9)	-74(11)	41(5)
C(2A)	7872(12)	2010(11)	308(11)	54(5)
C(3A)	7985(15)	1237(14)	-301(10)	56(5)
C(4A)	8477(17)	1536(14)	-1292(12)	49(12)
C(5A)	8858(13)	2607(11)	-1674(12)	64(5)
C(6A)	8745(10)	3379(8)	-1065(9)	45(3)
C(1B)	7752(10)	2345(10)	485(8)	40(4)
C(2B)	7790(8)	1372(9)	532(10)	47(3)
C(3B)	8178(14)	1046(11)	-317(14)	56(6)

C(4B)	8528(17)	1693(14)	-1214(13)	70(12)
C(5B)	8490(14)	2666(13)	-1261(11)	72(7)
C(6B)	8102(11)	2992(10)	-412(10)	43(5)
C(7)	8984(6)	4563(7)	1757(6)	31(2)
C(8)	9767(9)	4230(8)	1919(8)	55(3)
C(9)	10455(13)	4601(13)	2801(10)	73(8)
C(10)	10360(14)	5306(15)	3522(12)	40(6)
C(11)	9577(12)	5639(13)	3360(11)	47(5)
C(12)	8889(8)	5268(10)	2478(8)	41(3)
C(7A)	8366(9)	4659(11)	2360(9)	37(4)
C(8A)	8895(11)	4039(11)	2176(9)	42(4)
C(9A)	9775(13)	4184(14)	2824(11)	46(6)
C(10A)	10126(15)	4948(15)	3658(11)	82(11)
C(11A)	9597(15)	5567(12)	3843(8)	42(4)
C(12A)	8717(11)	5423(11)	3194(8)	44(4)
C(7B)	8330(8)	3769(10)	2363(8)	40(4)
C(8B)	9280(10)	3697(9)	2504(10)	39(3)
C(9B)	10126(12)	4453(13)	3146(13)	51(6)
C(10B)	10022(12)	5280(15)	3648(15)	56(8)
C(11B)	9072(11)	5352(13)	3507(14)	57(6)
C(12B)	8226(10)	4596(12)	2865(10)	45(4)
C(20)	7029(11)	3250(50)	5443(9)	150(20)
Cl(21)	7063(3)	2882(2)	4706(3)	75(1)
Cl(22)	6882(11)	3497(14)	6723(2)	132(4)

5.3. Unit cells of 2 and 3

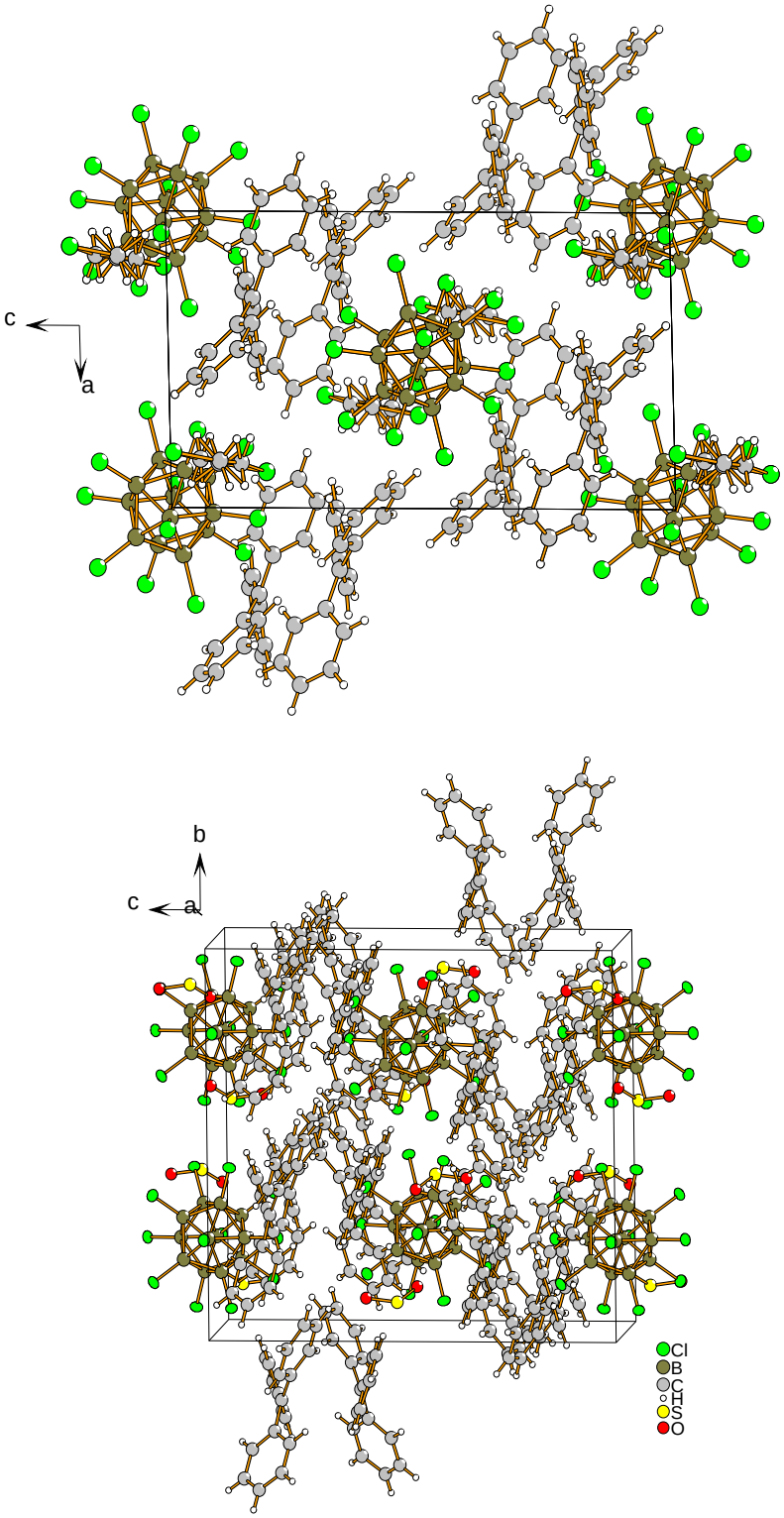

Fig. S25 Unit cells of **2** (top) and **3** (bottom).

6. References

1. J. R. Durig, W. H. Green, A. L. Marston, *J. Mol. Struct.*, 1968, **2**, 19.
2. K. G. Myakishev, I. I. Gorbacheva and V. V. Volkov, *Russ. J. Inorg. Chem.*, 1984, **29**, 526; *Zhur. Neorg. Khim.*, 1984, **29**, 912.
3. a) B. Brellochs and H. Binder, *Angew. Chem.*, 1988, **100**, 270-271; *Angew. Chem. Int. Ed. Engl.*, 1988, **27**, 262-263; b) B. Brellochs and H. Binder, *Z. Naturforsch.*, 1988, **43b**, 648.
4. a) T. Renner, *Angew. Chem.*, 1957, **69**, 478; b) *F. Klanberg, H. W. Kohlschütter, Chem. Ber.*, 1961, **94**, 786; c) B. Albert and K. Schmitt, *Z. Anorg. Allg. Chem.*, 2001, **627**, 809.
5. a) G. F. Freeguard and L. M. Long, *Chem. Ind. (London, U. K.)*, 1965, 471; b) M. Periasamy, *Organoboranes for Syntheses, ACS Symp. Ser. Vol. 783* (P. V. Ramachandran and H. C. Brown, Eds.), p. 65-78, American Chemical Society, Washington, DC, 2001.
6. K. C. Nainan and G. E. Ryschkewitsch, *Inorg. Nucl. Chem. Lett.*, 1970, **6**, 765, b) K. C. Nainan and G. E. Ryschkewitsch, *Inorg. Synth.*, 1974, **15**, 113.
7. a) I. A. Ellis, D. F. Gaines and R. Schaeffer, *J. Am. Chem. Soc.*, 1963, **85**, 3885; b) L. V. Titov, E. R. Eremin, V. Y. Rosolovskii, *Russ. J. Inorg. Chem.*, 1982, **27**, 500; *Zhur. Neorg. Khim.*, 1982, **27**, 891.
8. a) F. Klanberg and E. L. Muetterties, *Inorg. Chem.*, 1966, **5**, 1955; b) J. M. Makhlouf, W. V. Hough and G. T. Hefferan, *Inorg. Chem.*, 1967, **6**, 1196; c) L. Titov, M. D. Levicheva and S. B. Psikha, *Russ. J. Inorg. Chem.*, 1984, **29**, 386; *Zhur. Neorg. Khim.*, 1984, **29**, 668; d) W. Preetz and G. Peters, *Eur. J. Inorg. Chem.*, 1999, 1831.
9. In contrast to (F. Wang, Y. Wang and X. Wang, *Yingyong Huaxue (Chin. J. Appl. Chem.)*, 1998, **15**, 111) we were only able to precipitate part of the boric acid. The solubility of boric acid in water is reduced by addition of HCl. At 26 °C still about 0.6

mol boric acid are soluble in 2 mol/L hydrochloric acid: *Gemlins Handbuch der Anorganischen Chemie*, System-Nummer 13, Bor, 8th ed., Verlag Chemie, 1926.

10. The crystal structure of $Cs_2[B_{12}H_{12}]$ has been determined. I. Tiritiris, T. Schleid, K. Müller and W. Preetz, *Z. Anorg. Allg. Chem.*, 2000, **626**, 323.

11. The solubility of $M_2[B_{12}H_{12}]$ in water at 25 °C has been determined to be 44.7 mass% for Li^+, 50.7 mass% for Na^+, 41,3 mass% for K^+, 9.1 mass% for Rb^+, and 2.7 mass% for Cs^+. Zhukova, N. A., Malinina, E. A., Kuznetsov and N. T.: *Russ. J. Inorg. Chem.*, 1985, **30**, 735; *Zhur. Neorg. Khim.*, 1985, **30**, 1292.

12. a) H. D. B. Jenkins, H. K. Roobottom, J. Passmore and L. Glasser, *Inorg. Chem.*, 1999, **38**, 3609, b) L. Glasser and H. D. B. Jenkins, *Chem. Soc. Rev.*, 2005, **34**, 866.

13. S. I. Gryzlow, I. P. Goldshtein, *Russ. J. Phys. Chem*., 1989, **63**, 903-904; *Zh. Fiz. Khim.,* 1989, **63**, 1637.

14. *Gaussian 03, Revision C.02*, M. J. Frisch, G. W. Trucks, H. B. Schlegel, G. E. Scuseria, M. A. Robb, J. R. Cheeseman, J. A. Montgomery, Jr., T. Vreven, K. N. Kudin, J. C. Burant, J. M. Millam, S. S. Iyengar, J. Tomasi, V. Barone, B. Mennucci, M. Cossi, G. Scalmani, N. Rega, G. A. Petersson, H. Nakatsuji, M. Hada, M. Ehara, K. Toyota, R. Fukuda, J. Hasegawa, M. Ishida, T. Nakajima, Y. Honda, O. Kitao, H. Nakai, M. Klene, X. Li, J. E. Knox, H. P. Hratchian, J. B. Cross, V. Bakken, C. Adamo, J. Jaramillo, R. Gomperts, R. E. Stratmann, O. Yazyev, A. J. Austin, R. Cammi, C. Pomelli, J. W. Ochterski, P. Y. Ayala, K. Morokuma, G. A. Voth, P. Salvador, J. J. Dannenberg, V. G. Zakrzewski, S. Dapprich, A. D. Daniels, M. C. Strain, O. Farkas, D. K. Malick, A. D. Rabuck, K. Raghavachari, J. B. Foresman, J. V. Ortiz, Q. Cui, A. G. Baboul, S. Clifford, J. Cioslowski, B. B. Stefanov, G. Liu, A. Liashenko, P. Piskorz, I. Komaromi, R. L. Martin, D. J. Fox, T. Keith, M. A. Al-Laham, C. Y. Peng, A. Nanayakkara, M. Challacombe, P. M. W. Gill, B. Johnson, W.

Chen, M. W. Wong, C. Gonzalez and J. A. Pople, Gaussian, Inc., Wallingford CT, 2004.

15. M. F. C. Ladd and W. H. Lee, *J. Inorg. Nucl. Chem.*, 1959, **11**, 264.

16. I. Tiritiris and T. Schleid, *Z. Anorg. Allg. Chem.*, 2004, **630**, 1555.

17. D. W. M. Hofmann, *Acta Crystallogr*., 2002, **B57**, 489.

18. a) *TURBOMOLE Version 5.10*; COSMOlogic, b) R. Ahlrichs, M. Bär, M. Häser, H. Horn and C. Kölmel, *Chem. Phys. Let.*, 1989, **162**, 165.